

Femtosecond optical reflectivity measurements of lattice-mediated spin repulsions in photoexcited LaCoO₃ thin films

J. Bielecki,^{1,2,*} A. D. Rata,^{3,†} and L. Börjesson¹

¹*Department of Applied Physics, Chalmers University of Technology, SE-41296 Göteborg, Sweden*

²*Department of Cell and Molecular Biology, Uppsala University, Box 596, SE-75124 Uppsala, Sweden*

³*IFW Dresden, Institute for Metallic Materials, Helmholtzstraße 20, 01069 Dresden, Germany*

(Received 9 November 2012; revised manuscript received 29 December 2013; published 21 January 2014)

We present results on the temperature dependence of ultrafast electron and lattice dynamics, measured with pump-probe transient reflectivity experiments, of an epitaxially grown LaCoO₃ thin film under tensile strain. Probing spin-polarized transitions into the antibonding e_g band provides a measure of the low-spin fraction, both as a function of temperature and time after photoexcitation. It is observed that femtosecond laser pulses destabilize the constant low-spin fraction ($\sim 63\%$ – 64%) in equilibrium into a thermally activated state, driven by a subpicosecond change in spin gap Δ . From the time evolution of the low-spin fraction, it is possible to disentangle the thermal and lattice contributions to the spin state. A lattice mediated spin repulsion, identified as the governing factor determining the equilibrium spin state in thin-film LaCoO₃, is observed. These results suggest that time-resolved spectroscopy is a sensitive probe of the spin state in LaCoO₃ thin films, with the potential to bring forward quantitative insight into the complicated interplay between structure and spin state in LaCoO₃.

DOI: [10.1103/PhysRevB.89.035129](https://doi.org/10.1103/PhysRevB.89.035129)

PACS number(s): 78.47.jg, 75.30.Wx, 75.70.-i, 78.20.Ls

I. INTRODUCTION

The transition-metal perovskite LaCoO₃ has attracted considerable attention as a consequence of its puzzling spin-state transitions [1–3]. In the ground state, LaCoO₃ is a diamagnetic insulator with rhombohedral space group $R\bar{3}c$ and low-spin (LS) d -orbital occupancy $t_{2g}^6 e_g^0$. With increasing temperature the spin state gradually transforms towards a paramagnetic state, which has been discussed to be of either intermediate spin (IS) $t_{2g}^5 e_g^1$ ($S = 1$) or high-spin (HS) $t_{2g}^4 e_g^2$ ($S = 2$) character.

The driving mechanism behind the spin-state transition has been attributed to the sensitive interplay between the crystal field splitting Δ_{CF} , the intraionic exchange energy Δ_U , and the e_g bandwidth W , via the spin-gap $\Delta = \Delta_{CF} - W/2 - \Delta_U$ found to be ~ 200 K (17 meV) in magnitude. Δ allows a thermally depopulated low-spin fraction according to Fermi statistics [4,5];

$$n_{LS}(T) = \frac{1}{1 + Z \exp(-\Delta/T)}, \quad (1)$$

where $Z = (2S + 1)\eta$ is the combined spin and orbital degeneracy of the excited state.

It was realized early on by Goodenough [2,3] that the ionic size difference between the small LS and large HS Co³⁺ ions can stabilize a 1:1 LS-HS ratio in a checkerboard pattern, where cooperative lattice effects act as a spin repulsion (SR) that prohibits further HS occupation. However, the observed n_{LS} exhibit neither the simple activation according to Eq. (1) nor the 1:1 LS-HS ratio at elevated temperatures. Instead, lattice interactions have been discussed as affecting n_{LS} , for example, in terms of an effective temperature-dependent spin

gap [6] or “negative cooperativity” [7]; where Δ increases with the number of HS sites, n_{HS} , through an energy of mixing between LS and HS sites.

Recently, a ferromagnetic (FM) state with HS character even at low temperature was observed in epitaxially grown LaCoO₃ thin films [8–15]. The HS character is closely connected to substrate induced strain; polycrystalline thin films grown on Si substrates do not exhibit an FM HS ground state [8,11]. Moreover, x-ray absorption spectroscopy (XAS) complemented by atomic multiplet calculations indicates that epitaxial thin-film LaCoO₃ grown on SrTiO₃ (STO) have a constant LS fraction $n_{LS} = 0.64$ in the temperature range 10–300 K [15,16], in contrast to bulk LaCoO₃ as discussed above. The first experimental observations of a low-temperature HS state in strained LaCoO₃ thin films were discussed in terms of an increase in orbital overlap as the epitaxial strain increases the Co–O–Co angles [8,9,15]. Calculations [17] and a recent XAS study [18] instead emphasize the structural deformations as the driving mechanism behind the substrate-dependent HS fraction.

Lattice interactions are thus expected to be an important factor in the realized spin states, both in thin-film and bulk LaCoO₃. In this paper, we investigate the lattice contributions to n_{LS} in thin film LaCoO₃ using femtosecond transient reflectivity measurements. Time-resolved pump-probe spectroscopy provides a powerful technique for directly investigating the electron, lattice, and spin dynamics on a subpicosecond time scale and has previously been used to temporally disentangle the origins of many unique properties of transition metal oxides [19–21]. Here, we show that n_{LS} can be measured by probing magneto-optical transitions in thin-film LaCoO₃. It is observed that the underlying n_{LS} follows the purely thermal activation [Eq. (1)], while the time evolution of n_{LS} reveals a lattice mediated spin repulsion, as first proposed by Goodenough [2]. We argue that the SR is responsible for the deviations from a thermal spin population, both in the equilibrium and photoexcited states.

*johanb@xray.bmc.uu.se

†Present address: Max Planck Institute for Chemical Physics of Solids, Nöthnitzerstraße 40, DE-01187 Dresden, Germany.

II. EXPERIMENTAL

The LaCoO_3 thin film with thickness of 100 nm was epitaxially and coherently grown on a STO substrate by pulsed laser deposition. The in-plane lattice parameter of the LaCoO_3 film is identical with the substrate one, thus the LaCoO_3 film is fully strained and exhibits a FM state below 85 K. Above 85 K, the ferromagnetic order disappears and a paramagnetic state is instead observed up to at least 300 K. Details about the growth, structural, and magnetic characterization can be found elsewhere [11].

Time-resolved reflectivity measurements were performed at near normal incidence with a Ti:sapphire mode-locked amplifier with a 1-kHz repetition rate and 150-fs pulse duration. The p -polarized pump beam was set to 777 nm (1.6 eV), while the probe beam, obtained from the s -polarized second harmonic signal from a β -BBO crystal, was fixed at the second harmonic wavelength 388 nm (3.2 eV). The pump and probe wavelengths were chosen to match the broad magneto-optical transitions centered at 1.5 and 3.1 eV, respectively [22]. The beam diameters at the sample surface were adjusted to 135 and 160 μm for the probe and pump, respectively, giving a constant pump fluence $<1 \text{ mJ}/\text{cm}^2$, resulting in ~ 0.03 absorbed photons/Co site and a probe/pump fluence ratio of less than 1/100.

III. RESULTS

Figure 1(a) shows the first 4 ps of the transient reflectivity normalized to the peak value at 300 K, dR_N , in the temperature interval 10–300 K. The initial rise of dR_N centered around 0 ps delay arises from the instantaneous hole-carrier excitation. After the initial photoexcitation, a fast decay from the thermalization of excited carriers is observed on the 100-fs time scale [23,24]. The amplitude of this decay is relatively weak at 300 K and increases rapidly below 100 K, see the time-temperature 2D plot in Fig. 1(b).

As the minimum in dR_N is reached, a second process takes over, see Fig. 1(c) where delays up to 20 ps are shown. This process is due to a combination of the nonthermal lattice relaxation (LR) previously seen in cobaltite systems [25] and the usual coherent acoustical phonons (CAPs) from its wavefront [26], propagating through the sample at the speed of sound. Notice also the lack of significant changes in the dynamics between 10–100 K, where mainly a translational offset due to increased strength of the subpicosecond decay is observed with decreasing temperature.

After 17 ps, the LR and CAPs reach the substrate as indicated by discontinuity at the broken line in Fig. 1(d) where dR_N up to 200 ps is shown. The persistent oscillations show that the CAPs continue into the bulk of STO with a frequency of 113 GHz as inferred from the power spectrum in the inset. We obtain a speed of sound $C_{\text{LCO}} = 5.9$ and $C_{\text{STO}} = 9.0 \text{ km/s}$, respectively.

The probe pulse at 3.2 eV is in resonance with the spin-polarized and formally dipole-forbidden $t_{2g} \rightarrow e_g^*$ transition centered at 3.1 eV, from O $2p$ derived to Co d derived bands [22]. However, Co–O hybridization effects make this transition dipole-allowed [22], and the observed features in dR_N are thus sensitive to the density of empty e_g^* states and,

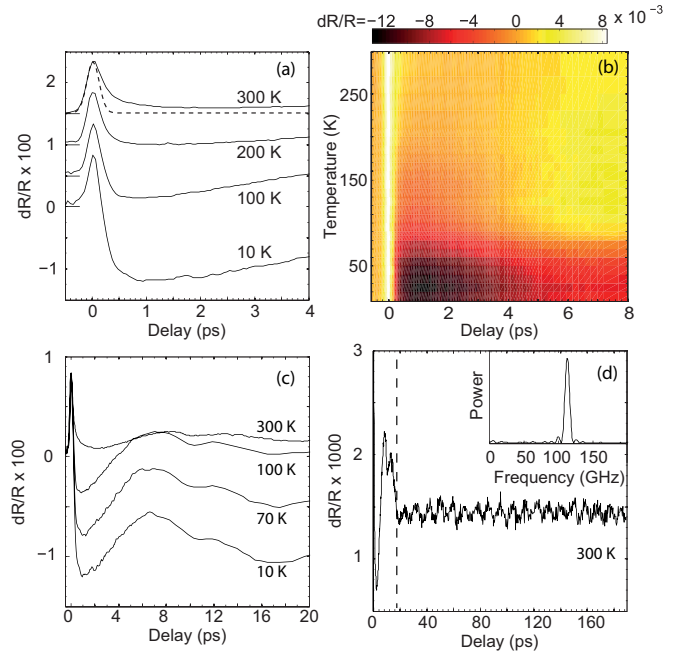


FIG. 1. (Color online) Transient reflectivity of a LaCoO_3 thin film under tensile strain in the temperature range 10–300 K. Each transient is normalized to the 300 K peak value at 0 ps. (a) shows transients at 300, 200, 100, and 10 K. The broken line is the pump pulse autocorrelation and indicates the achievable time resolution. For clarity, each transient has been offset along the y axis, with the respective zero-level indicated by the leftmost solid line. In (b), transients for all measured temperatures are collected in a 2D plot with dR/R given by the color bar. (c) Transient reflectivity in the 0–20 ps range. (d) dR/R at 300 K for 0–200 ps. From the constant magnitude of dR_N after 20 ps, we conclude that the photoinduced change in the spin state is long lived, returning to equilibrium as the holes and carriers recombine.

consequently, to n_{LS} , which in its purest form follows the thermally activated behavior in Eq. (1).

To visualize the time and temperature evolution of $n_{\text{LS}}(T, \tau)$, we make vertical cuts in Fig. 1(b) at different delays τ . The cut taken at $\tau = 500 \text{ fs}$ [see the red circles in Fig. 2(a)] is fitted well to Eq. (1), both with a HS $S = 2$ model where $\Delta = 200 \pm 10 \text{ K}$ and $Z = 5$ (solid line) and with an IS $S = 1$ model, where $\Delta = 175 \pm 8 \text{ K}$ and $Z = 3$ (broken line), and it is from these fits that the numerical $n_{\text{LS}}(T, \tau)$ values are extracted. Based on previous experimental [15,16] and computational [14] works, we adopt the HS interpretation in the following discussions. The excellent fit of Eq. (1) to the data is the first verification that dR_N indeed contain information about n_{LS} . At larger τ , the thermal evolution of n_{LS} begins to deviate from the thermally activated state. Here, a rapid increase of n_{LS} towards the equilibrium low-spin fraction $n_{\text{eq}} = n_{\text{LS}}(T, \infty)$ is observed for $T \geq 100 \text{ K}$, while below 100 K, we observe an n_{LS} independent on τ , see Fig. 2(a). The static n_{LS} below 100 K can also be observed directly in the experimental dR_N data as the previously mentioned invariant shape below 100 K seen in Fig. 1(c).

The increase in n_{LS} as a function of delay at 300 K is highlighted in Fig. 2(b) where n_{LS} is plotted as a function of τ ,

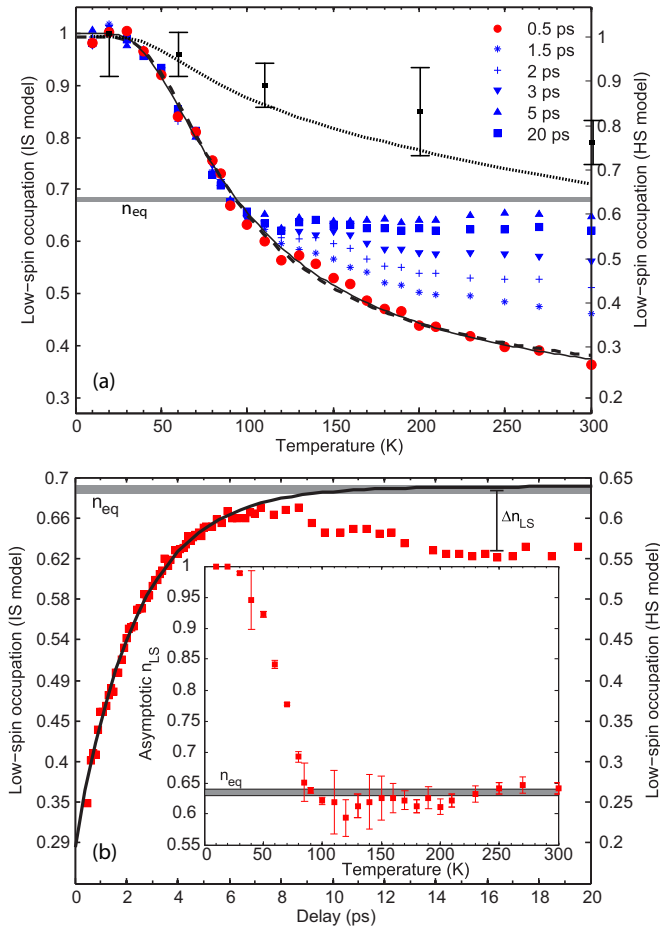


FIG. 2. (Color online) (a) The temperature and time-dependent low-spin fraction $n_{LS}(T, \tau)$, extracted from the measured dR/R as explained in the text, for six different time delays. Bulk data from Ref. [6] are shown with the black squares and error bars together with the calculated n_{LS} from Ref. [30] (dotted line). (b) A vertical cut at 300 K, showing the complete time evolution of $n_{LS}(300 \text{ K}, \tau)$ (red squares) after subtraction of oscillations from CAPs. An exponential (solid line) provides a good fit to the initial increase of $n_{LS}(300 \text{ K}, \tau)$. In the inset, the electron-lattice equilibrium LS fraction obtained from the exponential fit is shown for all temperatures. The HS model gives an average of 62.5%, in agreement with the previously estimated $n_{eq} = 0.63\text{--}0.64$ (shaded areas) [15,16].

after the removal of an oscillatory component from the LR and CAPs [26]. n_{LS} increases rapidly between 0.5 and 8 ps before a slow decrease sets in. The rapid increase can be described with a simple exponential that asymptotically reaches the equilibrium value $n_{LS} = 0.64$ with time constant $\tau_{e-l} = 2.8$ ps, typical for electron-lattice (e-l) relaxations [23,24,27–29]. The decrease in n_{LS} after 8 ps is attributed to the LR process discussed above [25].

In the inset of Fig. 2(b), the asymptotic n_{LS} , with error bars indicating a 95% confidence interval, obtained in this way is plotted for all temperatures. Above 90 K, n_{LS} varies between 60% and 64% and these variations can at least partly be assigned to uncertainties arising from the exponential fitting and removal of the oscillatory CAP signal. The fact that we obtain a constant n_{eq} with the same value as reported elsewhere [15,16]

provides a nontrivial consistency check of our results and interpretation of the pump-probe signal. However, it should be noted that it is in general not possible to extract $n_{LS}(T, \tau)$ from $dR_N(T, \tau)$ without additional constraints. In particular, we expect it to be difficult to extend the methodology used here to interpret analogous experiments performed on bulk LaCoO_3 . For thin-film LaCoO_3 , the possibility to extract the absolute $n_{LS}(T, \tau)$ hinges on the fact that n_{eq} has been reported to be constant in the 10–300-K temperature range [15,16], although we stress that the actual numerical value of n_{eq} was not used as input in obtaining $n_{LS}(T, \tau)$.

IV. DISCUSSION

Our observations can be explained as follows. The photoexcitation with 1.6-eV photons is in resonance with the magneto-optical transition at 1.5 eV and excites electrons into the Co derived e_g^* band [22,25], creating hole-carrier pairs with a quasistable concentration during the remainder of our measurements [24]. The observed effect is a pump pulse intensity dependent increase of Δ , leading to a ferromagnet to diamagnet collapse of the equilibrium n_{LS} into a distribution following a purely thermal activation [red circles in Fig. 2(a)]. As this process occurs on a subpicosecond time scale, we assign this increase of Δ to an electronic process where the creation of holes decreases the orbital overlap and O $2p$ -Co $3d$ bandwidth.

Below 100 K, n_{LS} follows an essentially static thermal occupation that relaxes back to n_{eq} as the equilibrium Δ is recovered on the hole-carrier recombination time scale. Above 100 K, n_{LS} increases towards n_{eq} on the e-l relaxation time scale and we interpret this as a lattice mediated SR, through cooperative oxygen displacements to accommodate the large HS Co^{3+} ions. From the abrupt crossover from thermally excited to SR saturated n_{LS} at 100 K, we deduce that the effective strength of the SR is zero above a critical n_{LS} , below which the SR becomes strong enough to completely negate further thermal LS depopulation in the temperature range investigated here. This argument is summarized in Fig. 3.

After e-l relaxation but before carrier-hole recombination, the observed spin states are remarkably similar to the idealized model describing bulk LaCoO_3 proposed by Goodenough, which incorporates a thermally activated n_{LS} until the SR stabilizes a checkerboard $n_{LS} = 0.5$ arrangement [2,3,30]. The discrepancy between the predicted $n_{LS} = 0.5$ and the observed $n_{LS} = 0.64$ implies that it is necessary to take into account collective electron-lattice interactions beyond the nearest-neighbor approximation to fully understand the SR and we expect these interactions to be sensitive to the detailed crystal structure and thus strain.

Indeed, a clear dependence of the SR on the strain state is observed in Fig. 2(b) from the decrease Δn_{LS} in n_{LS} above 8 ps due to the increased strain from the LR, which temporarily decreases the lattice interactions by acting as negative pressure [25]. From a comparison between the 0.5- and 20-ps LS distributions below 100 K in Fig. 2(a), it can be seen that Δ is not affected by the LR, i.e., the SR is decoupled from the spin gap magnitude.

The equilibrium thin-film state can now be understood as having a suppressed Δ due to strain induced lattice

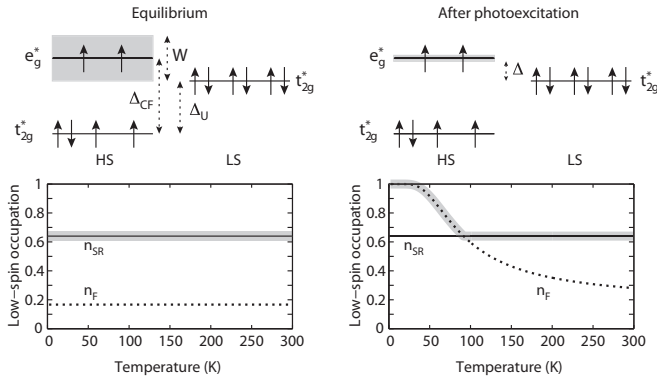


FIG. 3. Schematic over the effect of photoexcitation on n_{LS} . The upper left panel shows the relative energies [31] in a hypothetical equilibrium state where $\Delta = 0$, including the crystal-field splitting Δ_{CF} , the intra-atomic exchange energy Δ_U and the p - d bandwidth W . The resulting n_{LS} , shown in the lower left panel (shaded area), is constant and constrained by the SR (solid line) as opposed to the Fermi distribution n_F (broken line). The experimentally observed $n_{eq} = 0.64$ above 10 K is consistent with $\Delta \leq 20$ K. Photoexcitation (upper right panel) decrease W to give an increased Δ . In this case, n_{LS} follows the Fermi distribution n_F until the low-spin fraction given by the SR is reached (lower right panel). For clarity, both the magnitude and change in W is greatly exaggerated.

deformations, whereby the SR determines n_{LS} down to at least 10 K. This constrains Δ to ≤ 20 K. Because the SR is very sensitive to the structural properties of the thin film, different n_{LS} and consequently magnetization strengths are observed on different substrates [8,11]. Further, the constant SR observed in the thin film could be explained by a quenching of the anomalous lattice expansion that couples to the spin state in bulk LaCoO_3 [32,33] by epitaxial adhesion to the substrate. This explanation of the variations in magnetization on different substrates in terms of the SR is in accord with the recent XAFS study by Sterbinsky *et al.* [18] where it was argued that structural distortions are the important parameters for stabilizing the HS phase rather than the strength of the orbital hybridization.

Our conclusions supplement previous interpretations of the spin-state evolution in bulk LaCoO_3 , where a temperature dependent spin gap $\Delta(T)$, influenced by lattice relaxations, was used to explain the deviations from a thermally excited spin fraction [6,7]. While temperature induced variations of the lattice parameters are expected to affect Δ via the p - d bandwidth and Co–O bond length [31], we here demonstrate the decoupling of $\Delta(T)$ and the significant contribution to n_{LS} from the SR. As shown in the strain-induced low-spin decrease Δn_{LS} [see Fig. 2(b)], the SR strength should also be expected to vary with strain and temperature. This suggests that n_{LS} in bulk LaCoO_3 [shown in Fig. 2(a), squares with error bars [6] and dotted line [30]] is determined by a temperature dependent interplay between Δ and the SR.

V. SUMMARY AND CONCLUSIONS

In summary, we have presented time-resolved pump-probe measurements on LaCoO_3 , where irradiation with a femtosecond 1.6-eV laser pulse causes an increase in Δ , which initiates a ferromagnet to diamagnet transition occurring at the subpicosecond time scale. Probing the magneto-optical transition at 3.2 eV, we are able to disentangle the thermal from the lattice contributions to n_{LS} and measure the ultrafast spin-state evolution.

We observe a lattice mediated spin repulsion and argue that this effect determines the value of the n_{LS} and, consequently, the ferromagnetic moment, in tensile strained LaCoO_3 thin films. Even though lattice interactions have been widely suggested as affecting n_{HS} in LaCoO_3 [2,3,6,30,32], to our best knowledge, this is the first time these effects have been observed directly. Further time-resolved studies are needed to provide a clear understanding of the spin repulsion mechanism, which could assist in unraveling the spin-state transition in LaCoO_3 .

ACKNOWLEDGMENTS

We are grateful to Ezio Zanghellini for valuable discussions and technical assistance. JB and LB acknowledge the generous financial support from the Swedish Research Council (VR).

-
- [1] M. Imada, A. Fujimori, and Y. Tokura, *Rev. Mod. Phys.* **70**, 1039 (1998).
 - [2] J. B. Goodenough, *J. Phys. Chem. Solids* **6**, 287 (1958).
 - [3] M. A. Senariz-Rodríguez and J. B. Goodenough, *J. Solid State Chem.* **116**, 224 (1995).
 - [4] S. W. Biernacki, *Phys. Rev. B* **74**, 184420 (2006).
 - [5] A. Ishikawa, J. Nohara, and S. Sugai, *Phys. Rev. Lett.* **93**, 136401 (2004).
 - [6] M. W. Haverkort, Z. Hu, J. C. Cezar, T. Burnus, H. Hartmann, M. Reuther, C. Zobel, T. Lorenz, A. Tanaka, N. B. Brookes, H. H. Hsieh, H. J. Lin, C. T. Chen, and L. H. Tjeng, *Phys. Rev. Lett.* **97**, 176405 (2006).
 - [7] T. Kyômen, Y. Asaka, and M. Itoh, *Phys. Rev. B* **67**, 144424 (2003).
 - [8] D. Fuchs, C. Pinta, T. Schwarz, P. Schweiss, P. Nagel, S. Schuppler, R. Schneider, M. Merz, G. Roth, and H. von Loehneysen, *Phys. Rev. B* **75**, 144402 (2007).
 - [9] D. Fuchs, E. Arac, C. Pinta, S. Schuppler, R. Schneider, and H. von Loehneysen, *Phys. Rev. B* **77**, 014434 (2008).
 - [10] V. V. Mehta, M. Liberati, F. J. Wong, R. V. Chopdekar, E. Arenholz, and Y. Suzuki, *J. Appl. Phys.* **105**, 07E503 (2009).
 - [11] A. D. Rata, A. Herklotz, L. Schultz, and K. Dorr, *EPJ B* **76**, 215 (2010).
 - [12] J. W. Freeland, J. X. Ma, and J. Shi, *Appl. Phys. Lett.* **93**, 212501 (2008).
 - [13] A. Herklotz, A. D. Rata, L. Schultz, and K. Dorr, *Phys. Rev. B* **79**, 092409 (2009).
 - [14] H. Hsu, P. Blaha, and R. M. Wentzcovitch, *Phys. Rev. B* **85**, 140404 (2012).

- [15] M. Merz, P. Nagel, C. Pinta, A. Samartsev, H. v Loehneysen, M. Wissinger, S. Uebe, A. Assmann, D. Fuchs, and S. Schuppler, *Phys. Rev. B* **82**, 174416 (2010).
- [16] C. Pinta, D. Fuchs, M. Merz, M. Wissinger, E. Arac, H. Von Loehneysen, A. Samartsev, P. Nagel, and S. Schuppler, *Phys. Rev. B* **78**, 174402 (2008).
- [17] J. M. Rondinelli and N. A. Spaldin, *Phys. Rev. B* **79**, 054409 (2009).
- [18] G. E. Sterbinsky, P. J. Ryan, J. W. Kim, E. Karapetrova, J. X. Ma, J. Shi, and J. C. Woicik, *Phys. Rev. B* **85**, 020403 (2012).
- [19] C. Kübler, H. Ehrke, R. Huber, R. Lopez, A. Halabica, R. F. Haglund, Jr., and A. Leitenstorfer, *Phys. Rev. Lett.* **99**, 116401 (2007).
- [20] M. Rini, R. Tobey, N. Dean, J. Itatani, Y. Tomioka, Y. Tokura, R. W. Schoenlein, and A. Cavalleri, *Nature (London)* **449**, 72 (2007).
- [21] S. Dal Conte, C. Giannetti, G. Coslovich, F. Cilento, D. Bossini, T. Abebaw, F. Banfi, G. Ferrini, H. Eisaki, M. Greven, A. Damascelli, D. van der Marel, and F. Parmigiani, *Science* **335**, 1600 (2012).
- [22] S. Yamaguchi, Y. Okimoto, K. Ishibashi, and Y. Tokura, *Phys. Rev. B* **58**, 6862 (1998).
- [23] A. J. Sabbah and D. M. Riffe, *Phys. Rev. B* **66**, 165217 (2002).
- [24] S. Sundaram and E. Mazur, *Nat. Mater.* **1**, 217 (2002).
- [25] Y. Okimoto, X. Peng, M. Tamura, T. Morita, K. Onda, T. Ishikawa, S. Koshihara, N. Todoroki, T. Kyômen, and M. Itoh, *Phys. Rev. Lett.* **103**, 027402 (2009).
- [26] C. Thomsen, H. T. Grahn, H. J. Maris, and J. Tauc, *Phys. Rev. B* **34**, 4129 (1986).
- [27] R. D. Averitt, A. I. Lobad, C. Kwon, S. A. Trugman, V. K. Thorsmolle, and A. J. Taylor, *Phys. Rev. Lett.* **87**, 017401 (2001).
- [28] T. Ogasawara, K. Tobe, T. Kimura, H. Okamoto, and Y. Tokura, *J. Phys. Soc. Jpn.* **71**, 2380 (2002).
- [29] J. Bielecki, R. Rauer, E. Zanghellini, R. Gunnarsson, K. Dörr, and L. Börjesson, *Phys. Rev. B* **81**, 064434 (2010).
- [30] T. Kyômen, Y. Asaka, and M. Itoh, *Phys. Rev. B* **71**, 024418 (2005).
- [31] J. S. Zhou, J. Q. Yan, and J. B. Goodenough, *Phys. Rev. B* **71**, R220103 (2005).
- [32] S. Murata, S. Isida, M. Suzuki, Y. Kobayashi, K. Asai, and K. Kohn, *Physica B* **263**, 647 (1999).
- [33] C. Zobel, M. Kriener, D. Bruns, J. Baier, M. Gruninger, T. Lorenz, P. Reutler, and A. Revcolevschi, *Phys. Rev. B* **66**, 020402 (2002).